



# Quercetin-loaded solid lipid nanoparticles exhibit antitumor activity and suppress the proliferation of triple-negative MDA-MB 231 breast cancer cells: implications for invasive breast cancer treatment

Mahdi Hatami<sup>1,2</sup> · Maryam Kouchak<sup>3,4</sup> · Alireza Kheirollah<sup>2</sup> · Layasadat Khorsandi<sup>1</sup> · Mojtaba Rashidi<sup>1,2</sup> 

Received: 4 March 2023 / Accepted: 26 September 2023 / Published online: 13 October 2023  
© The Author(s), under exclusive licence to Springer Nature B.V. 2023

## Abstract

**Background** Quercetin (QC) is a naturally occurring flavonoid found in abundance in fruits and vegetables. Its anti-cancer and anti-inflammatory properties have been previously demonstrated, but its low bioavailability hampers its clinical use. Triple-negative breast cancer is a subtype of breast cancer with a poor response to chemotherapy. This study investigates the anti-cancer effects of quercetin-solid lipid nanoparticles (QC-SLN) on the triple-negative breast cancer cell line MDA-MB231.

**Materials and methods** MCF-7 and MDA-MB231 cells were treated with 18.9  $\mu$ M of QC and QC-SLN for 48 h. Cell viability, apoptosis, colony formation assay, and the anti-angiogenic effects of the treatment were evaluated.

**Results** QC-SLN displayed optimal properties (particle size of 154 nm, zeta potential of  $-27.7$  mV, encapsulation efficiency of 99.6%, and drug loading of 1.81%) and exhibited sustained release of QC over 72 h. Compared to the QC group, the QC-SLN group showed a significant decrease in cell viability, colony formation, angiogenesis, and a substantial increase in apoptosis through the modulation of Bax and Bcl-2 at both gene and protein levels. The augmentation in the proportion of cleaved-to-pro caspases 3 and 9, as well as poly (ADP-ribose) polymerase (PARP), under the influence of QC-SLN, was conspicuously observed in both cancer cell lines.

**Conclusions** This study showcases quercetin-solid lipid nanoparticles (QC-SLN) as a promising therapy for triple-negative breast cancer. The optimized QC-SLN formulation improved physicochemical properties and sustained quercetin release, resulting in reduced cell viability, colony formation, angiogenesis, and increased apoptosis in the MDA-MB231 cell line. These effects were driven by modulating Bax and Bcl-2 expression, activating caspases 3 and 9, and poly (ADP-ribose) polymerase (PARP). Further *in vivo* studies are needed to confirm QC-SLN's efficacy and safety.

---

✉ Mojtaba Rashidi  
ms\_rashidi60@yahoo.com; rashidi-mo@ajums.ac.ir

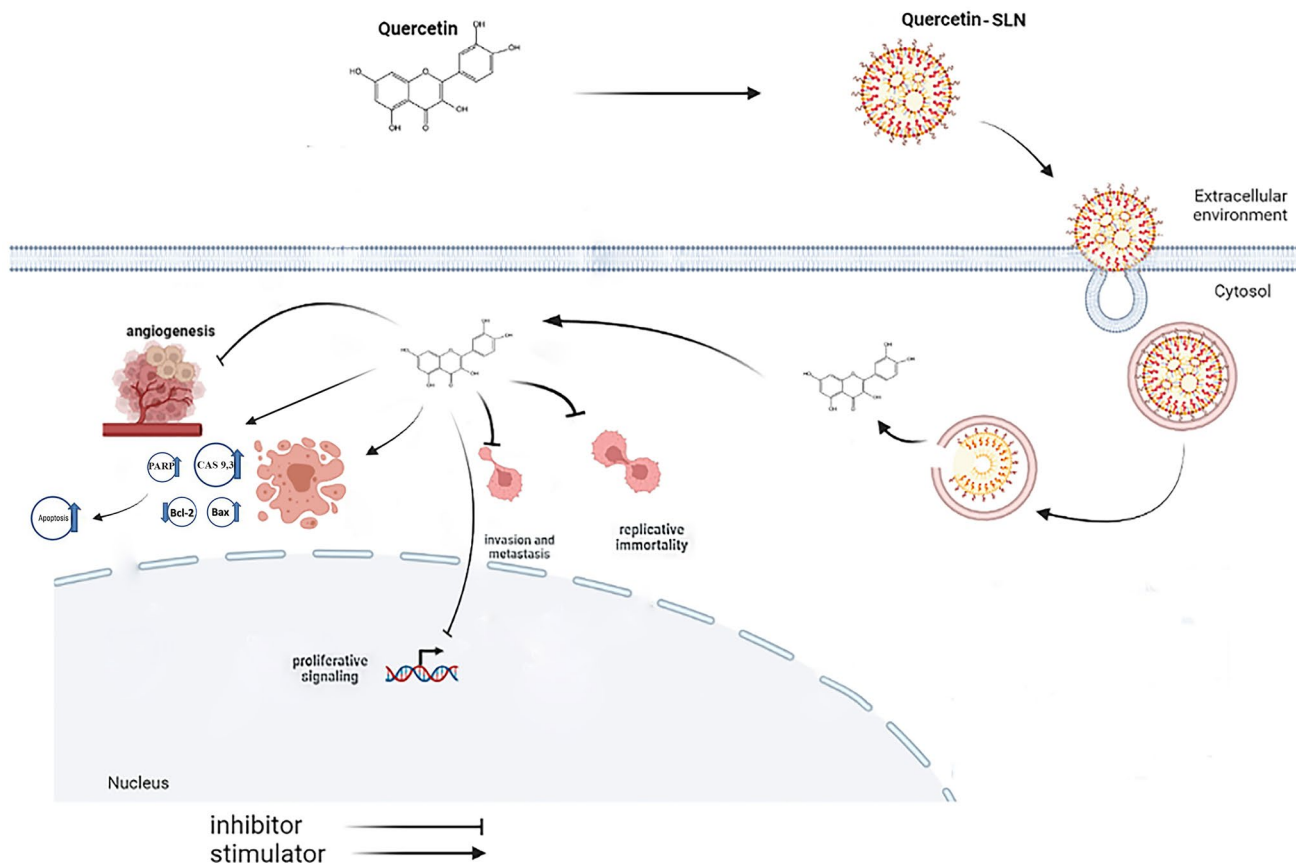
<sup>1</sup> Cellular and Molecular Research Center, Medical Basic Sciences Research Institution, Ahvaz Jundishapur University of Medical Sciences, Ahvaz, Iran

<sup>2</sup> Department of Clinical Biochemistry, Faculty of Medicine, Ahvaz Jundishapur University of Medical Sciences, Ahvaz, Iran

<sup>3</sup> Nanotechnology Research Center, Ahvaz Jundishapur University of Medical Sciences, Ahvaz, Iran

<sup>4</sup> Department of Pharmaceutics, Faculty of Pharmacy, Ahvaz Jundishapur University of Medical Sciences, Ahvaz, Iran, Ahvaz Jundishapur University of Medical Sciences, Ahvaz, Iran

## Graphical abstract



**Keywords** Solid lipid nanoparticles (SLN) · Quercetin · Apoptosis · Invasive · Breast cancer

## Introduction

Cardiovascular disease is the leading cause of death globally, with cancer following as the second most common cause. Among various cancer types, breast cancer has emerged as a significant cause of cancer-related mortality among women and the most frequently diagnosed cancer worldwide. In 2020 alone, breast cancer accounted for approximately 14% of all female malignancies and led to the deaths of 685,000 women. Although chemotherapy and radiation therapy are potent treatments for breast cancer, they are associated with several side effects [1–4]. Consequently, recent research efforts have focused on identifying safe and effective natural remedies to mitigate these complications [5–7].

Quercetin (QC), a potent flavonoid with anti-inflammatory and anti-cancer properties, can be found in a variety of fruits and vegetables, such as citrus fruits, apples, radish leaves, and red onions. Previous studies have demonstrated that QC exhibits cytotoxic effects on numerous cancer cell types [8–13]. However, the clinical applications

of QC have been limited due to its low solubility and poor bioavailability [14, 15]. To overcome these limitations, researchers have developed various drug delivery systems, including liposomes, polymers, and solid lipid nanoparticles (SLNs), which could enhance solubility and bioavailability. Recent studies have particularly focused on employing SLNs as carriers for both chemical and natural drugs, including flavonoids [16–22]. For instance, tamoxifen-loaded SLNs have been shown to effectively reduce breast cancer [23], and pomegranate extract-loaded SLNs can efficiently inhibit the growth of various cancer cells, such as those in prostate, breast, and liver cancers [24]. SLNs can enhance drug effectiveness by protecting the drug from chemical degradation, increasing its half-life, and facilitating slow release [25–27].

While several investigations have been conducted on the anti-tumor effects of various natural remedies in SLN-loaded formulations [23], the cytotoxic mechanisms underlying these effects have received less attention. Overcoming cancer cells' resistance to apoptosis is a significant

challenge in cancer treatment; therefore, any therapeutic strategy that can address drug resistance will be valuable. Previous studies have shown that drugs loaded with SLN could partially overcome drug resistance, suggesting that this type of treatment could improve the success of drug therapy. The present study aimed to investigate the cytotoxic and apoptotic effects of quercetin-loaded SLNs (QC-SLNs) on highly invasive MDA-MB231 breast cancer cells.

Natural substances like quercetin can trigger apoptosis by modulating essential proteins in the apoptotic pathway. The regulation of Bcl-2 family proteins, including pro-apoptotic Bax and anti-apoptotic Bcl-2, is one such process that plays a critical role in determining cellular outcomes. Moreover, caspase activation, particularly for caspase-3 and caspase-9, is crucial initiating and carrying out apoptosis [28]. The cleavage of poly (ADP-ribose) polymerase (PARP), a target of caspase-3, marks the beginning of apoptosis [29]. By regulating apoptosis-inducing proteins, QC-SLN can demonstrate improved anticancer effectiveness and ultimately trigger apoptosis in cancer cells.

In light of this situation, our objective was to clarify the capacity of QC-SLNs to induce apoptosis and be cytotoxic in MDA-MB231 breast cancer cells, thereby addressing the knowledge gap concerning the cytotoxic processes involved. Consequently, we examined the regulation of crucial proteins in the apoptotic pathway by QC-SLNs, which may offer valuable information regarding their therapeutic potential in the treatment of breast cancer.

## Materials and methods

### Preparation of QC-SLN

4.75 g of Campritol 888 ATO (Glyceryl Dibehenate, Gattefossé, France) were heated to 75 °C and mixed with 100 mg of QC. In a separate beaker, 0.25 g of oleic acid and 0.5 g of lecithin were added to heated (80 °C) deionized water, stirred for 5 min, and then completely mixed with the previous solution using a sonicator (Elmasonic S60H, Global Industrial, USA). To generate the nanoemulsion, 4 mL of 1% polyvinyl alcohol (PVA) at 3 °C was added to the prior solution and homogenized at 10,000 rpm using a homogenizer (Heidolph, Germany). The suspension was centrifuged twice at 5 °C and 25,000 RCF for 20 min. The QC-SLNs were stored in sealed containers at refrigerated temperatures until used.

### Fourier transform infrared (FTIR)

Following QC loading into the SLN, the FTIR spectra (VERTEX 70v, Bruker, USA) were analyzed to confirm intermolecular interactions. Pellets were prepared by

compressing QC, QC-SLN, and blank-SLN at 200 kg/cm<sup>2</sup> with KBr. The FTIR spectra of the aforementioned materials were obtained in the range of 400–4,000 cm<sup>-1</sup> with a resolution of 1 cm<sup>-1</sup>.

### Transmission electron microscopy (TEM)

The morphology of the SLN was examined using transmission electron microscopy (TEM). A droplet of the SLN was placed onto a carbon-coated copper grid to form a thin liquid layer. Excess samples were collected on filter paper and allowed to air-dry at room temperature for 5 min. The morphology of the SLN was assessed using TEM (ZEISS LEO 906 E).

### Particle size and zeta potential

The average particle size, zeta potential, and polydispersity index (PDI) of QC-SLNs were analyzed by a nanosizer and a zetasizer (Malvern, England).

### Encapsulation efficiency (EE) and drug loading (DL)

To initially determine the encapsulation efficiency (EE), the separation of free (untrapped) quercetin (QC) from QC-solid lipid nanoparticles (SLN) in the suspension was performed by centrifugation at 25,000 rpm for 25 min. The QC content of the supernatant was then measured at 256 nm using a UV spectrophotometer. The EE was calculated using the following formula [30, 31].

$$EE(\%) = 100(D_i - D_f)/D_i.$$

Here,  $D_i$  and  $D_f$  represent the initial (total) and free (untrapped) drug concentrations, respectively. By dissolving QC-SLN in methanol and measuring its QC content with a spectrophotometer at 256 nm, it was possible to calculate the drug loading (DL):  $DL(\%) = 100(\text{loaded drug}/\text{weight of lipid})$ .

### In vitro drug release

The dialysis bag method (MW cut-off of 12,000 Da, Sigma-Aldrich, USA) [32] was employed to evaluate QC release from QC-SLNs in phosphate-buffered saline (PBS) (pH 7.42) as the receptor phase at 37 °C. Samples were collected at predetermined intervals (from 5 min to 72 h), and their QC content was assessed spectrophotometrically (Ultraspec 3000, Pharmacia Biotech, USA) at 256 nm.

## Cell culture

### Design of experiments

Breast cancer cell lines MCF-7 and MDA-MB231, along with MRC5 normal lung fibroblast cells, were cultured in Dulbecco's Modified Eagle Medium (DMEM) high glucose medium supplemented with streptomycin (100 U/mL), fetal bovine serum (FBS) (10%), and penicillin (100 mg/mL), and obtained from the Iranian Pasteur Research Center. The cells were maintained in an incubator at 37 °C, 95% humidity, and 5% CO<sub>2</sub>. Different concentrations of QC (0–400 µM), QC-SLN (based on QC concentration), and blank SLN (2.5–50 µM) were used to determine the IC<sub>50</sub> after 24 and 48 h of incubation.

### Cell viability

The MTT assay was utilized to evaluate the effect of the treatment on cell viability. After culturing breast cancer cells and MRC5 cells ( $4 \times 10^3$  cells/well) in 96-well plates for 24 and 48 h, each well was incubated with 0.5 mg/mL MTT solution for four hours at 37 °C. The supernatant was removed from each well, and 100 µL of dimethyl sulfoxide (DMSO) was added. The absorbance of the sample was then measured at 570 nm using an Elisa reader (BioTek, ELx800, USA).

### Clonogenic assay

The clonogenic assay was employed to assess the anti-proliferative effect of QC and QC-SLNs on MCF-7 and MDA-MB-231 cells. A total of 2000 cells were seeded into six-well plates and incubated with 18.9 µM of QC, QC-SLNs, and blank-SLN for MCF-7 and 13.4 µM of QC, QC-SLNs, and blank-SLN for MDA-MB 231 for 48 h. The medium containing treatments was then replaced with fresh complete media (DMEM with 10% FBS plus 1% penicillin/streptomycin) without any treatment, and the cells were grown for 14 days. The colonies were fixed with formaldehyde, stained with 0.5% crystal violet in PBS, and counted using a light microscope.

### Flow cytometry analysis

A total of  $4 \times 10^5$  MCF-7 and MDA-MB-231 cells were cultured in a six-well plate and treated with QC and QC-SLN for 48 h. Following this, the percentage of normal, apoptotic, and necrotic cells was determined using the Annexin V-FITC/Propidium iodide assay kit (IQ Products, Rozenburglaan, Netherlands) according to the

manufacturer's instructions. In brief, the cell pellets were resuspended in 200 µl of binding buffer after rinsing with PBS, and 5 µl of Annexin V-FITC was incubated with 5 µl of Propidium iodide (PI) for 10 min. The samples were then diluted to 200 µl with binding buffer and analyzed using a flow cytometer (Becton Dickinson, San Jose, California, USA).

### Real-time polymerase chain reaction

In accordance with the manufacturer's instructions,  $1 \times 10^6$  cells were utilized for RNA extraction, and total RNA was isolated using RNX-Plus Solution. The purity and integrity of the RNA were assessed by the A260/A280 ratio and agarose gel electrophoresis. The isolated RNA was stored at -70 °C in 50 µl of DEPC-treated water. A cDNA synthesis kit was employed to perform reverse transcription in a 20 µl reaction mixture, following the manufacturer's protocol. SYBR Green qPCR Master Mix (Yekta Tajhiz Azuma, Tehran, Iran) was used to quantify Bax, Bcl-2, and GAPDH gene expression. The PCR program was executed as follows: 10 min at 96 °C, 40 cycles of 15 s at 95 °C, 30 s at 60 °C, and 34 s at 60 °C. GAPDH served as a housekeeping gene for normalizing expression levels. Fold changes were calculated using the  $2^{(-\Delta\Delta CT)}$  method. Primer sequences are provided in Supplementary Table S1.

### Western blot analysis

Treated breast cancer cells were thoroughly washed in cold PBS (pH 7.42) and subsequently harvested in a RIPA (radioimmunoprecipitation) lysis solution containing protease inhibitors. After performing SDS-PAGE and blotting, the PVDF membrane was blocked with 5% non-fat milk. The membrane was then incubated with primary antibodies for 24 h and secondary antibodies for 1 h. Primary (anti-Bax, anti-Bcl-2, anti-Caspases 8, 9, 3, anti-PARP, and anti- $\alpha$ -Tubulin antibodies) and secondary antibodies were obtained (Santa Cruz Biotechnology and Cell Signaling Technology Inc., USA). Protein bands were visualized using the ECL kit (Abcam, USA), and band density was determined using Image J software (National Institutes of Health, Bethesda, United States).

### Chorioallantoic membrane assay (CAM assay)

The CAM assay was conducted to assess angiogenesis in vivo. Chicken eggs, provided by Ahvaz University's Department of Poultry, were randomized and divided into four groups (control, blank SLN, QC, and QC-SLN 130 µM; n=3 per group) and incubated at 37 °C with 55–60% humidity. On day three of incubation, a 1–2 cm square window was created on the top of each viable eggshell, and

1.5 ml of albumin was removed from the opposite side of the eggs. As chorioallantoic membrane (CAM) maturation occurs on day five, drug-loaded sterile methylcellulose discs were placed on the CAMs at that time. The eggs were incubated for an additional 48 h following drug administration. After the removal of filter discs, CAM tissue was fixed in 4% formaldehyde, and images were captured at 150× magnification using a stereomicroscope (Leica Zoom 2000). The Wimasis Image Analysis Software, available online, was employed for image analysis. Angiogenesis was evaluated based on the total vessel branch points and total vessel network lengths.

### Statistical analysis

Each experiment was performed independently three times, and results are presented as mean ± standard deviation (SD). GraphPad Prism 8 (California, USA) was utilized for statistical analysis. Experimental group findings were compared using one-way ANOVA and LSD posthoc tests, with P values < 0.05 considered significant.

## Results

### FTIR

As seen in Supplementary Fig. 1, multiple distinct bands exist in the QC-SLN spectra, including O–H stretching ( $3850$  to  $3200$   $\text{cm}^{-1}$ ), C–O stretching ( $1635$   $\text{cm}^{-1}$ ), C–C stretching ( $1659$   $\text{cm}^{-1}$ ), C–H bending ( $1463$ ,  $1379$   $\text{cm}^{-1}$ ), C–O stretching inside the ring structure ( $1262$   $\text{cm}^{-1}$ ), and

C–O stretching the ring structure ( $1109$ – $1056$   $\text{cm}^{-1}$ ). The FTIR spectra confirm the interaction between QC and SLN.

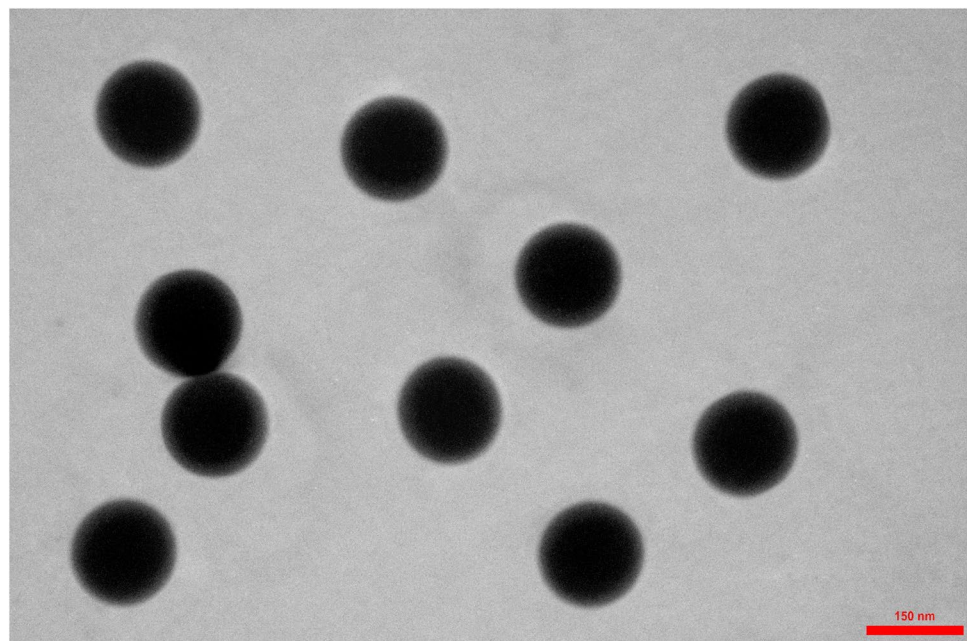
### Characterization of QC-SLNs

The negative zeta potential of the nanoparticles was approximately  $-27.7$  mV, preventing aggregation and ensuring long-term stability. The PDI value for QC-SLN was  $0.50 \pm 0.04$ , indicating a uniform distribution of nanoparticles. Encapsulation efficiency was 99.6%, and drug loading was 1.81%. Transmission electron microscope (TEM) images revealed that the nanoparticles were spherical and smooth (Fig. 1), with an average size of  $154 \pm 22.5$  nm. This size corresponds with particle sizes obtained via dynamic light scattering (DLS), which measured 156 nm. The data demonstrated that the majority of particles were smaller than 156 nm.

### Drug release profile

Supplementary Figure 2 demonstrates that the release characteristics of the quercetin (QC) solution differ significantly from those of the QC-loaded solid lipid nanoparticles (QC-SLN). While the QC solution exhibits rapid drug release, reaching approximately 100% within 5 h, the QC-SLN displays a sustained release profile that continues for 3 days. Within the first 12 h, QC-SLN releases 65% of the QC, and over the subsequent 72 h, the release gradually increases to 90%.

**Fig. 1** The TEM micrograph of QC-SLN. Scale bar: 150 nm





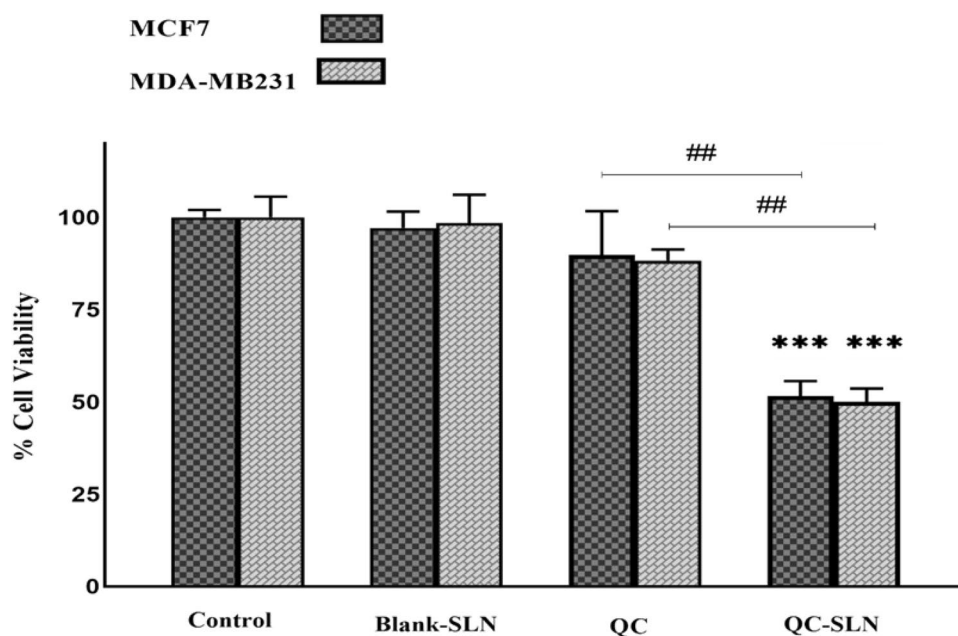
## Cell viability and proliferation

The viability of two cancer cell lines (MCF-7 and MDA-MB-231) and one normal cell line (MRC-5) was assessed after 24 and 48 h of treatment with QC (20–400  $\mu\text{M}$ ), QC-SLN (2.5–50  $\mu\text{M}$ , based on QC), and Blank-SLN (0.2–6.66 mg/ml) using an MTT assay. Supplementary Fig. 3 displays the results, and the  $\text{IC}_{50}$  values are presented in Supplementary Table S2. Notably, the concentrations for the blank were chosen based on the lipid concentration in the QC-SLNs used in the preparation of concentrations of 20–400  $\mu\text{M}$  (based on QC). As depicted in Supplementary Fig. 3, both QC and QC-SLN decrease the viability of cancer cells without significantly affecting normal cell viability at concentrations below 50  $\mu\text{M}$ . Blank-SLN does not impact cell viability in either cancerous or normal cells. The  $\text{IC}_{50}$  values of QC-SLN (Supplementary Table S2) for MCF-7 and MDA-MB231 after 48 h of treatment are 18.9  $\mu\text{M}$  and 13.4  $\mu\text{M}$ , respectively (Fig. 2).

## Clonogenic assay

Figure 3 A presents photographs of MCF-7 and MDA-MB231 colony formation in untreated and treated conditions. The quantification of colony formation assays in both cell lines is depicted in Fig. 3B and C. For both cell lines, Blank-SLN has an insignificant effect on colony formation, and QC-SLN significantly decreases the colony number compared to the QC group.

**Fig. 2** Cell viability of MCF-7 and MDA-MB231. The MTT assay was used to determine cell viability after 48 h treatment with 18.9  $\mu\text{M}$  of Blank SLN, QC, and QC-SLN for MCF-7 and 13.4  $\mu\text{M}$  of Blank SLN, QC, and QC-SLN for MDA-MB-231. The data were shown as mean  $\pm$  SD. \*\*\* $P < 0.001$  against control group and ## $P < 0.01$  against QC group are considered as significant



## Annexin V-FITC/propidium iodide apoptosis assay

Figure 4 shows that in the free QC treatment, a high percentage of necrotic cells is observed in both MCF-7 (76.9%) and MDA-MB231 (55.3%) cell lines. Blank-SLN has no apoptotic effect on the cells. QC increases the apoptosis rate in MCF-7 by approximately 7.5% and in MDA-MB231 by 10.09%. QC-SLN significantly enhances the apoptotic effect on MCF-7 and MDA-MB231 compared to QC by 29.38% and 40.41%, respectively.

## Quantitative real-time RT-PCR

In MCF-7 cells, blank-SLN has an insignificant influence on gene expression. In the QC group, increased gene expression of Bax is observed without any significant effect on Bcl-2 expression compared to the control group. In QC-SLN, a considerable reduction in the gene expression of Bcl-2 and an increase in Bax expression compared to the QC group are observed (Fig. 5A). In MDA-MB231 cells, no significant change in gene expression is seen in the Blank-SLN and QC groups. However, under QC-SLN treatment, significant decreases and increases in Bcl-2 and Bax gene expression compared to the QC group are revealed, respectively (Fig. 5B).

## Western analysis

Figures 6 and 7 demonstrate that Blank-SLN does not exert a considerable influence on protein expression in either cell type. Figure 6A displays the protein expression of PARP, caspases 8, 9, 3, Bcl-2, and Bax in MCF-7 cells. In this

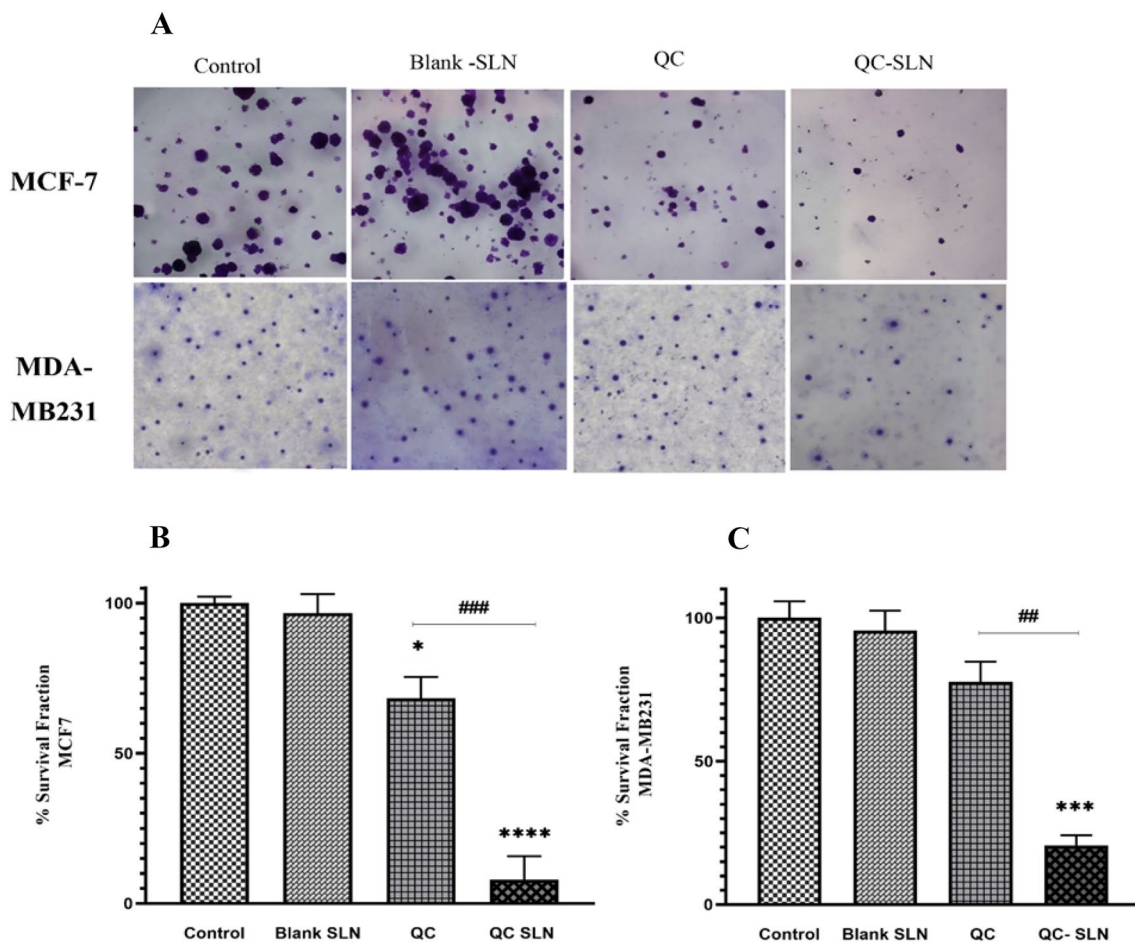


**Fig. 3** Colony formation assay of MCF-7 and MDA-MB231. Photograph of colony formation of both cell lines in the untreated and treated groups with blank SLN, QC, and QC-SLN for 48 h (A). The mean  $\pm$  SD of colony number in the untreated and treated groups was

determined using ImageJ (B and C). \*  $P < 0.05$ , \*\*\* $P < 0.001$ , and \*\*\*\* $P < 0.0001$ ; compared with the control group, ##  $P < 0.01$ , ###  $P < 0.001$  compared with the QC group

instance, Blank-SLN does not significantly affect protein expression. In the QC group, a rise in Bax protein expression can be observed without a notable alteration in PARP, caspases 8, 9, 3, and Bcl-2 levels. Contrarily, the QC-SLN group exhibits a marked increase in PARP, caspases 9, 3, Bax expression, and a decrease in Bcl-2 expression without a significant change in caspase 8 when compared to both the control and QC groups (Fig. 6B).

Figure 7A illustrates the protein expression of PARP, caspases 8, 9, 3, Bcl-2, and Bax in MDA-MB231 cells. In this case, no significant changes in protein expression are observed in the Blank-SLN and QC groups. Nevertheless, the QC-SLN group shows significant increases in PARP, caspases 9, 3, Bax expression, and decreases in Bcl-2 expression when compared to the control and QC groups. However, the expression of caspase 8 in the QC-SLN group remains unaltered relative to the control and QC groups (Fig. 7B).

### CAM assay analysis

The anti-angiogenic potential of QC-SLN and QC was assessed using the chorioallantoic membrane (CAM) assay. Figure 8A displays the angiogenesis of the CAM assay in different groups in the first row and the interpretation of these data by the Wimasis program in the second row. Following treatments, the same pattern is observed in both angiogenesis indices: total number of branch points and total length of the vessel network (Fig. 8B and C). The patterns indicate that QC and QC-SLN treatments result in a considerable reduction of these markers compared to the control. The proportion of this reduction is significantly higher in the QC-SLN treatment compared to the QC group.

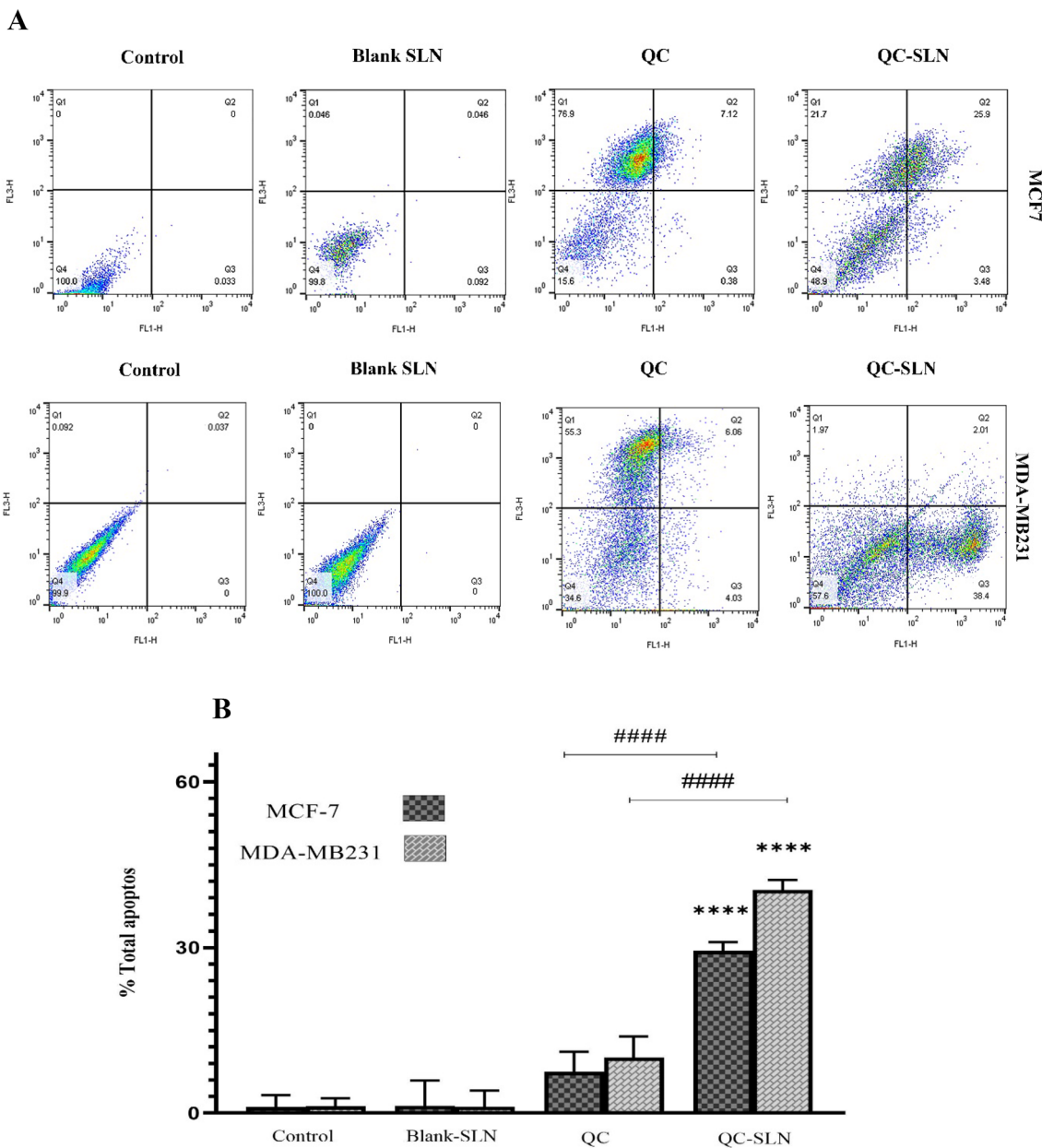


**Fig. 4** Flow cytometry analysis of apoptosis in MCF-7 and MDA-MB231. The assays used the IC<sub>50</sub> values, which were 18.9 μM for MCF-7 and 13.4 μM for MDA-MB231 cancer cells. Dot plot charts of flow cytometry analysis for control, Blank-SLN, QC, and QC-SLN

(A). Quantification of total apoptotic effect (late and early) in control and treatments (B). Data is shown as mean ± SD. \*\*\*\* *P* < 0.0001 compared with control group, #### *P* < 0.0001 compared with QC group

**Discussion**

In the current study, quercetin (QC) was effectively incorporated into solid lipid nanoparticles (SLN) using the emulsification method. The resulting QC-SLN exhibited remarkable stability and a uniform size distribution. The in vitro release profile demonstrated a sustained release of QC throughout the treatment period. This sustained release is anticipated to enhance quercetin’s bioavailability

and, consequently, its therapeutic efficacy. Our findings are consistent with previous research [30, 33], showing that QC-SLN significantly increased the bioavailability of quercetin, making it an ideal candidate for sustained drug release in cancer therapy, particularly breast cancer treatment.

Our results indicate that QC-SLN successfully reduced the total number of MCF-7 and MDA-MB231 cells by inhibiting cell growth and inducing cell death. Previous



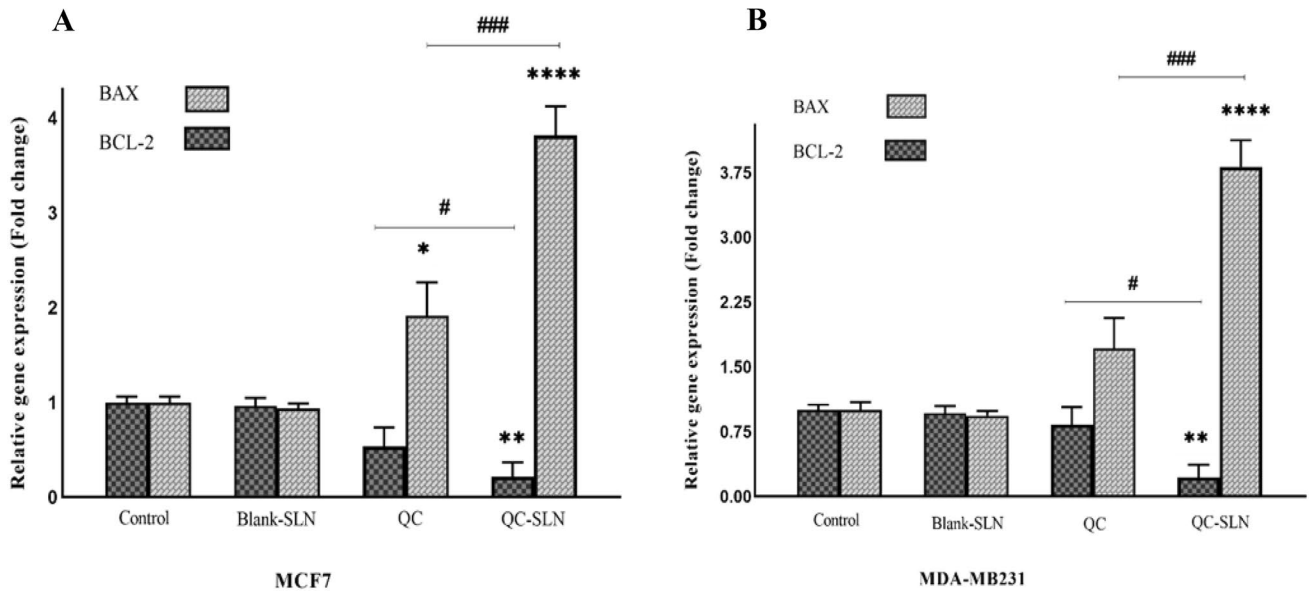


**Fig. 5** Gene expression of Bax and Bcl-2 in MCF-7 and MDA-MB231. Gene expression of Bax and Bcl-2 without or with treatments (Blank-SLN, QC, and QC-SLN) in MCF-7 (A) and MDA-

MB231 (B). Data shown as mean  $\pm$  SD. \* $P < 0.05$ , \*\* $P < 0.01$ ; \*\*\*\* $P < 0.0001$  compared to the control group; and #  $P < 0.05$ , ### $P < 0.001$  compared to the QC group

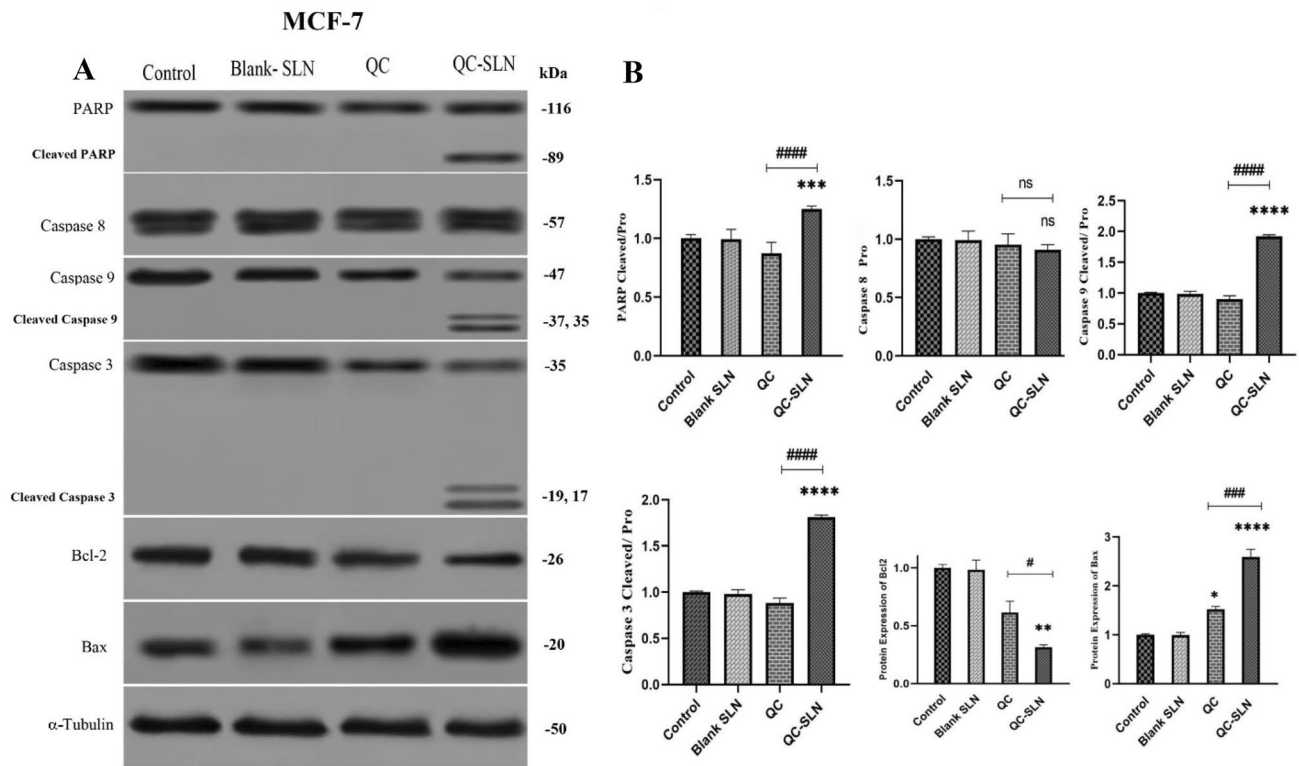


**Fig. 6** Protein expression of PARP, caspases 8, 9, 3 Bcl-2 and Bax in MCF-7. Protein bands PARP, caspases 8, 9, 3 Bcl-2 and Bax in MCF-7 (A) and quantification of protein expression of PARP, caspases 8, 9, 3 Bcl-2 and Bax in MCF-7 (B). The data was shown as the

mean  $\pm$  SD. \*\*\* $P < 0.001$ ; \*\*\*\* $P < 0.0001$  compared to the control group. ### $P < 0.001$ , #### $P < 0.0001$  compared to the QC group

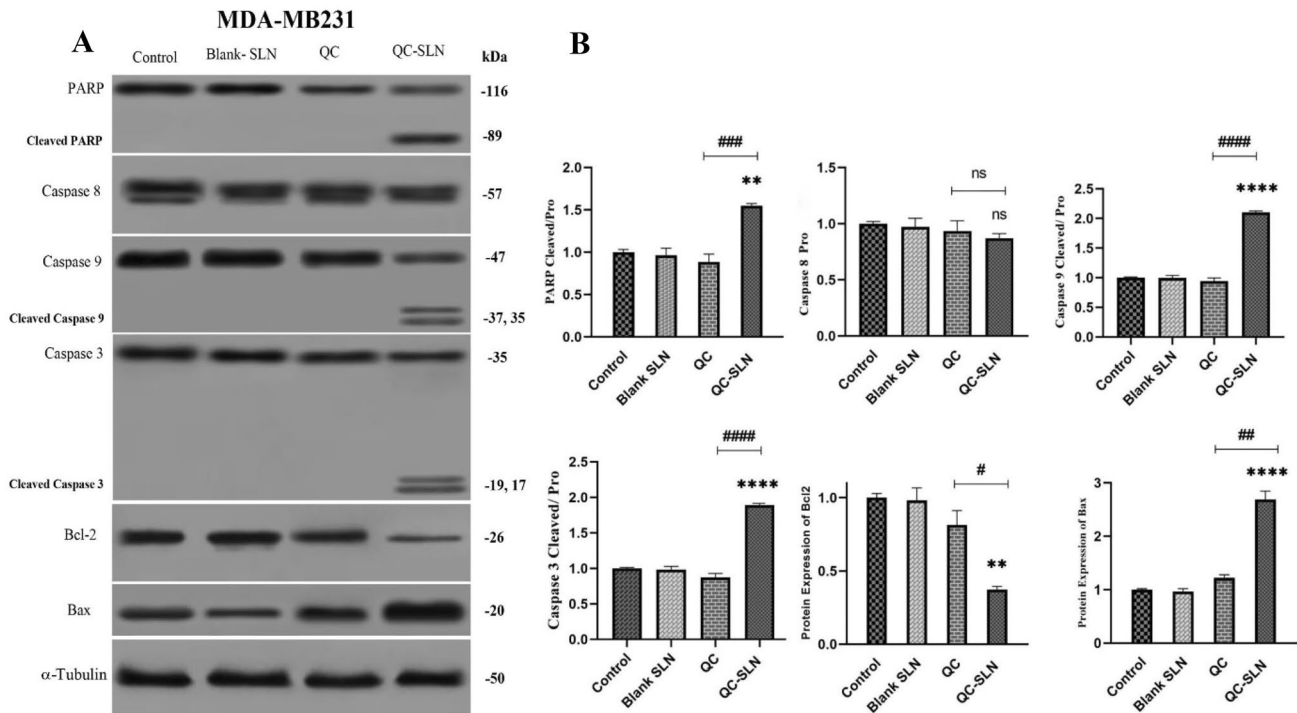


**Fig. 7** Protein expression of PARP, caspases 8, 9, 3 Bcl-2 and Bax in MDA-MB231. Protein bands PARP, caspases 8, 9, 3 Bcl-2 and Bax in MDA-MB231 (A) and Quantification of protein expression of PARP, caspases 8, 9, 3 Bcl-2 and Bax in MDA-MB231 (B). The

data was shown as the mean  $\pm$  SD. \*\* $P < 0.01$ ; \*\*\*\* $P < 0.0001$  compared to the control group. #  $P < 0.05$ , ##  $P < 0.01$ , ###  $P < 0.001$ , ####  $P < 0.0001$  compared to the QC group

studies have reported the inhibitory effect of QC on the viability of these cells [34–36]. According to our findings, the  $IC_{50}$  concentrations of QC after 48 h of treatment were 93  $\mu$ M and 183  $\mu$ M for MCF-7 and MDA-MB-231 cells, respectively. Our  $IC_{50}$  result for MCF-7 deviates slightly from the data published by Lin et al. (2013) and Firoozeh Niazvand et al. (2018), which could be attributed to differences in QC purity and quality [33, 34]. The  $IC_{50}$  values of QC-SLNs on MCF-7 and MDA-MB 231 were 18.9  $\mu$ M and 13.4  $\mu$ M, respectively, which are considerably lower than the  $IC_{50}$  values of QC alone. This finding suggests that QC-loaded nanoparticles exerted a stronger cytotoxic effect on MCF-7 and MDA-MB231 cells without significantly impacting MRC5.

Numerous studies have demonstrated that SLN serves as an effective carrier for anticancer drugs and flavonoids. Berberine, oridonin, and resveratrol encapsulated in SLNs exhibited enhanced antitumor effects on breast cancer cell lines [19, 36–38]. Zhuang et al. (2012) reported that breast cancer treatment with anticancer drugs loaded into SLN, such as mitoxantrone and methotrexate, could be more effective than treatment with the drugs alone [36]. Conversely, Abbasalipourkabir et al. (2016) showed that tamoxifen loaded into SLNs had a similar effect on breast cancer in rats as free tamoxifen [39]. More recently,

Firoozeh Niazvand et al. (2019) demonstrated that QC-loaded SLNs had a stronger impact on breast cancer than QC alone [33]. This phenomenon could be attributed to the lipophilic nature of the carrier, which promotes cellular uptake and consequently enhances the growth-inhibitory effect of QC-SLNs on cancer cells. In a study conducted by Vijayakumar et al., QC-SLN improved the solubility of QC in distilled water, and SLN significantly increased the cellular uptake of QC [30]. Sun et al. (2014) found that QC-loaded lipid carriers significantly improved the solubility and stability of QC, resulting in an increased presence of QC in MCF-7 cells. Their findings revealed that enhanced cytotoxicity was accompanied by increased QC uptake by MCF-7 cells [22].

The clonogenic assay results indicated that QC reduced the colony counts of MCF-7 and MDA-MB231 cells by 35% and 25%, respectively, while these reductions for QC-SLN were 90% and 80% for MCF-7 and MDA-MB231 cells, respectively. This finding further supports the enhanced efficacy of QC-SLN compared to QC alone. Our results are in line with previous research, which demonstrated that QC-SLN significantly reduced colony numbers compared to both control and QC [33].

Apoptosis and cell viability are commonly used methods to assess the effectiveness of anti-tumor drugs. In many

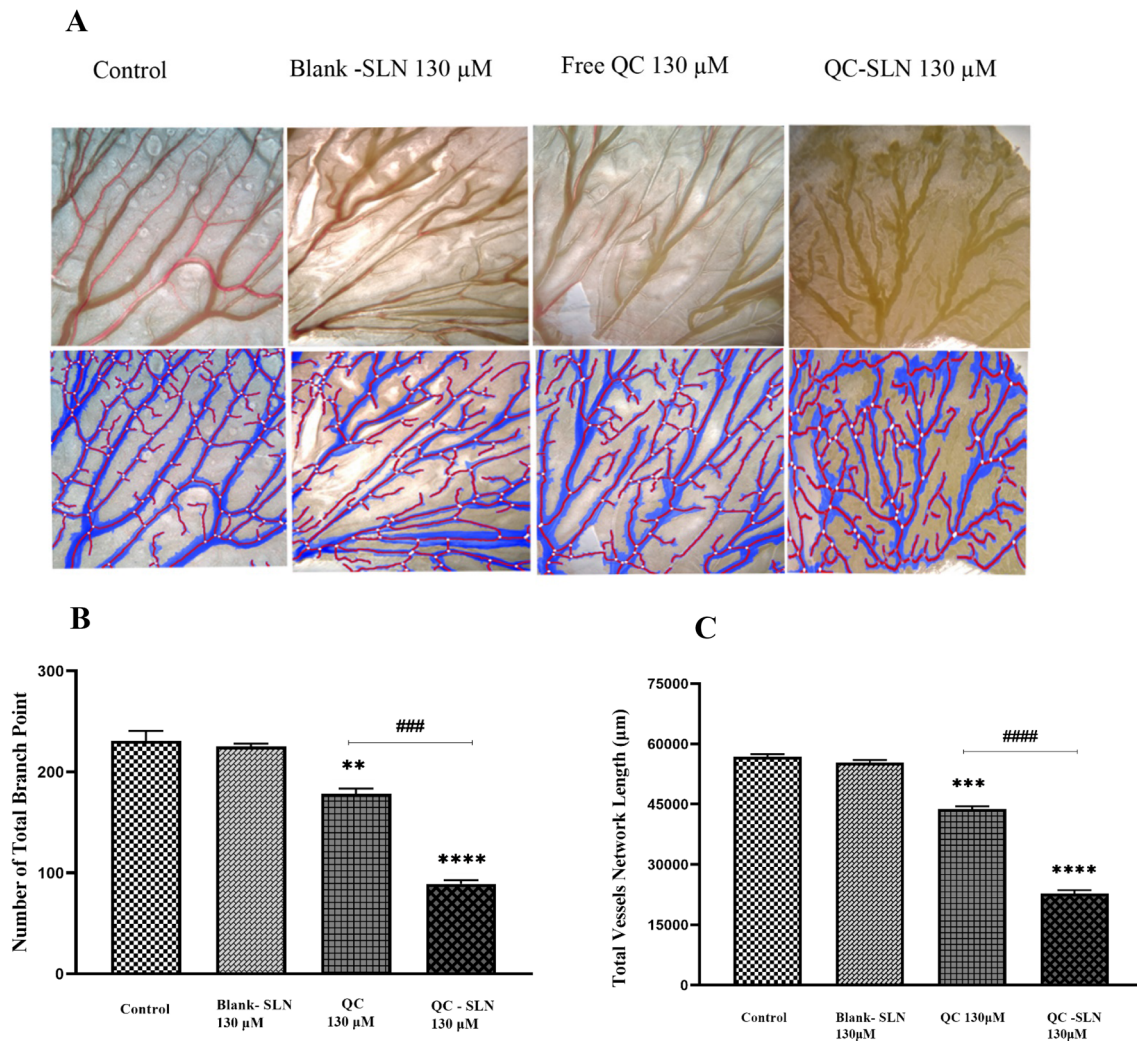


**Fig. 8** The effect of QC and QC-SLN on CAM angiogenesis. The first row shows the image of angiogenesis in control and 130  $\mu$ M of Blank-SLN, QC, and QC-SLN, and the second row shows the analysis of them with the Wimasis programme (A). Quantitative analysis of the anti-angiogenic effect of QC (130  $\mu$ M) and QC-SLN (130  $\mu$ M) based

on total branch points (B) and total vessel network length (C). The results are presented as the mean  $\pm$  SD of at least three independent experiments. \*\* $P$  < 0.01, \*\*\* $P$  < 0.001, and \*\*\*\* $P$  < 0.0001 compared with control, and ###  $P$  < 0.001, ####  $P$  < 0.0001 compared to the QC group

instances, anticancer drugs can destroy proliferating cells through apoptosis [40–42]. Our flow cytometry results demonstrated an increase in total apoptosis (early and late) in MCF-7 and MDA-MB231 cells treated with QC compared to the control group. This enhancement was significantly greater for QC-SLN than for QC alone. These findings are in agreement with previous studies by Jain et al. (2014) and Firoozeh Niazvand et al. (2019), which reported that QC-SLN promotes DNA damage and apoptosis in cancer cells [33, 43]. In our study, we found that free QC treatment resulted in a high percentage of necrotic cells in both MCF-7 and MDA-MB231 cell lines. This observation could be attributed to the cytotoxicity of free quercetin, which may induce oxidative stress and interfere with cellular functions, ultimately leading to necrosis [44]. Additionally, the cellular

uptake and intracellular distribution of free quercetin might differ from QC-SLN, further contributing to the observed differences in cell death modes [45]. Our findings are in line with those from Haghiaei M. et al. (2005), who discovered that QC causes both necrosis and apoptosis in SCC-9 oral cancer cells and breast cancer cells [33, 46].

To confirm apoptosis, we assessed the gene and protein expression of Bax and Bcl-2, two key regulatory proteins of the intrinsic apoptosis pathway [33]. In both breast cancer cell lines, QC increased Bax expression and decreased Bcl-2 at gene and protein levels. These changes in expression were more pronounced in QC-SLN treatment than in QC alone. As a result, QC-SLNs might potentially promote the intrinsic apoptotic pathway in breast cancer cells, leading to cell death. This part of our study's findings aligns with those

of Lee et al. (2008), who discovered that QC played a role in the pathway leading to apoptosis in prostate cancer cells [47]. Our results are also consistent with Duo J et al. (2012), who showed that QC, through the modulation of Bax and Bcl-2 expression, can stimulate apoptosis in MCF-7 cells and inhibit their proliferation [48].

The findings of our research do not align with previous studies on caspase 8 [49]. This discrepancy may be attributed to the employment of QC-SLN in our investigation, which could have altered quercetin's bioavailability and cellular uptake, consequently impacting the activation of caspases. Nanoformulations have the potential to enhance the solubility, stability, and cellular internalization of compounds, as well as modify their interactions with target proteins and signaling pathways.

In our study, we observed an increase in the cleavage of caspases 3 and 9, as well as PARP, which is in agreement with previous research [50]. This suggests that QC-SLN likely stimulates the intrinsic apoptotic pathway, circumventing caspase-8 activation.

The regulation of cell survival and death is influenced by the cleavage of PARP, which has a role in both apoptosis and necrosis [51]. When PARP becomes hyperactivated due to significant DNA damage or oxidative stress, the cell's energy resources become depleted. This depletion can lead to the collapse of ion gradients, loss of membrane integrity, and ultimately, necrotic cell death [52, 53]. Research has demonstrated that the inhibition or genetic elimination of PARP-1 provides protection against necrosis, emphasizing its critical function in this form of cell death [54]. Our hypothesis, derived from flow cytometry data, suggests that the observed increase in late apoptosis and necrosis may result from PARP hyperactivation in response to DNA damage or oxidative stress.

We performed the chorioallantoic membrane (CAM) assay as an *in vivo* angiogenic test, and the number of total branch points and total vessel network lengths were employed as markers of angiogenesis to analyze the effects of QC and QC-SLN on angiogenesis. Treatment with QC resulted in a reduction in both angiogenic indices compared to the control group, although QC-SLN decreased the indices more substantially and significantly than QC. This finding is in line with the results of Sanaei et al. (2021), who demonstrated that QC reduced both indices, and this effect was confirmed with human umbilical vein endothelial cells (HUVECs) culture [55].

## Conclusion

Our study demonstrated the therapeutic potential of QC-SLN in overcoming resistance in breast cancer, particularly in enhancing the cytotoxic effect on MCF-7 and MDA-MB231 cells, the latter being triple-negative with invasive properties and resistance to chemotherapy. The QC-SLN encapsulation promotes apoptosis primarily through the intrinsic pathway, as evidenced by upregulated Bax, downregulated Bcl-2, and activated caspases 3, 9 and PARP while also significantly reducing angiogenesis, as shown by the CAM assay. These findings emphasize the multifaceted approach of QC-SLN, targeting apoptosis, angiogenesis, and bioavailability, and highlight the need for complementary *in vivo* experiments to further validate its efficacy in conquering resistance in triple-negative breast cancer.

**Supplementary Information** The online version contains supplementary material available at <https://doi.org/10.1007/s11033-023-08848-w>.

**Acknowledgements** The research was financially supported by grant number CMRC – 9914 from the Cellular and molecular research center, medical basic sciences research institute Ahvaz Jundishapur University of Medical Sciences, Ahvaz, Iran. This paper was extracted from PhD thesis of Mahdi Hatami.

**Author contributions** MR significantly contributed to the conceptualization and design of the work. MK and LK prepared and updated the material. AK: data analysis and interpretation. MH: the acquisition, interpretation, and analysis of data.

**Funding** The research was financially supported by the Cellular and Molecular Research Center of Ahvaz Jundishapur University of Medical Sciences (CMRC - 9914), Ahvaz, Iran.

**Data availability** The data and materials used and/or analyzed during the current study are available from the corresponding author on request.

## Declarations

**Conflict of interest** We have no conflict of interest to declare.

**Ethical approval** IR.AJUMS.REC.1399.509.

**Research involving human and/or animal participants** This article does not contain any studies with human participants or animals performed by any of the authors.

**Informed consent** All of the authors declare consent to participate and consent for the publication.

## References

1. Tinoco G, Warsch S, Glück S, Avancha K, Montero AJ (2013) Treating breast cancer in the 21st century: emerging biological therapies. *J Cancer* 4:117



2. Gadhwal M, Patil S, D’Mello P, Joshi U, Sinha R, Govil G (2013) Synthesis, characterisation and antitumour activity of some quercetin analogues. *Indian J Pharm Sci* 75:233
3. Gibellini L, Pinti M, Nasi M, Montagna JP, De Biasi S, Roat E et al (2011) Quercetin and cancer chemoprevention. *Evid Based Complement Altern Med*. <https://doi.org/10.1093/ecam/neq053>
4. Dar RA, Rasool M, Assad A (2022) Breast cancer detection using deep learning: datasets, methods, and challenges ahead. *Comput Biol Med* 149:106073
5. Lv W, Budke B, Pawlowski M, Connell PP, Kozikowski AP (2016) Development of small molecules that specifically inhibit the D-loop activity of RAD51. *J Med Chem* 59:4511–4525
6. Aiello F, Carullo G, Giordano F, Spina E, Nigro A, Garofalo A et al (2017) Identification of breast cancer inhibitors specific for G protein-coupled estrogen receptor (GPER)-expressing cells. *ChemMedChem* 12:1279–1285
7. Dandawate PR, Subramaniam D, Jensen RA, Anant S (2016) Targeting cancer stem cells and signaling pathways by phytochemicals: novel approach for breast cancer therapy. *Semin Cancer Biol* 40:192–208
8. Srivastava S, Somasagara RR, Hegde M, Nishana M, Tadi SK, Srivastava M et al (2016) Quercetin, a natural flavonoid interacts with DNA, arrests cell cycle and causes tumor regression by activating mitochondrial pathway of apoptosis. *Sci Rep* 6:1–13
9. Tummala R, Lou W, Gao AC, Nadiminty N (2017) Quercetin targets hnRNPA1 to overcome enzalutamide resistance in prostate cancer cells; quercetin targets hnRNPA1 and synergizes with enzalutamide. *Mol Cancer Ther* 16:2770–2779
10. Lamson DW, Brignall MS (2000) Antioxidants and cancer, part 3: quercetin. *A J Clin Med Ther* 5:196–208
11. Davis JM, Murphy EA, Carmichael MD (2009) Effects of the dietary flavonoid quercetin upon performance and health. *Curr Sports Med Rep* 8:206–213
12. Shakerian E, Afarin R, Akbari R, Mohammadtaghvaei NJMBR (2022) Effect of Quercetin on the fructose-activated human hepatic stellate cells, LX-2, an in-vitro study. *Mol Biol Rep* 49:2839–2845
13. Shakerian E, Akbari R, Mohammadtaghvaei N, Gahrooie MM, Afarin R (2022) Quercetin reduces hepatic fibrogenesis by inhibiting TGF- $\beta$ /Smad3 signaling pathway in LX-2 cell line. *Jundishapur J Nat Pharm Prod*. <https://doi.org/10.5812/jjnpp.113484>
14. Dhumale SS, Waghela BN, Pathak C (2015) Quercetin protects necrotic insult and promotes apoptosis by attenuating the expression of RAGE and its ligand HMGB1 in human breast adenocarcinoma cells. *IUBMB Life* 67:361–373
15. Rauf A, Imran M, Khan IA, ur-Rehman M, Gilani SA, Mehmood Z et al (2018) Anticancer potential of quercetin: a comprehensive review. *Phytother Res* 32:2109–2130
16. Abd-Rabou AA, Ahmed HHJA (2017) CS-PEG decorated PLGA nano-prototype for delivery of bioactive compounds: a novel approach for induction of apoptosis in HepG2 cell line. *Adv Med Sci* 62:357–367
17. Jain A, Garg NK, Jain A, Kesharwani P, Jain AK, Nirbhavane P et al (2016) A synergistic approach of adapalene-loaded nanostructured lipid carriers, and vitamin C co-administration for treating acne. *Drug Dev Ind Pharm* 42:897–905
18. Mombeini M, Saki G, Khorsandi L, Bavarsad N (2018) Effects of silymarin-loaded nanoparticles on HT-29 human colon cancer cells. *Medicina* 54:1
19. Wang W, Zhang L, Chen T, Guo W, Bao X, Wang D et al (2017) Anticancer effects of resveratrol-loaded solid lipid nanoparticles on human breast cancer cells. *Molecules* 22:1814
20. Balakrishnan S, Mukherjee S, Das S, Bhat FA, Raja Singh P, Patra CR et al (2017) Gold nanoparticles-conjugated quercetin induces apoptosis via inhibition of EGFR/PI3K/Akt-mediated pathway in breast cancer cell lines (MCF-7 and MDA-MB-231). *Cell Biochem Funct* 35:217–231
21. Govindaraju S, Rengaraj A, Arivazhagan R, Huh Y-S, Yun K (2018) Curcumin-conjugated gold clusters for bioimaging and anticancer applications. *Bioconjug Chem* 29:363–370
22. Abbasalipourkabir R, Salehzadeh A, Abdullah R (2016) Tamoxifen-loaded solid lipid nanoparticles-induced apoptosis in breast cancer cell lines. *J Exp Nanosci* 11:161–174
23. Hwang JH, Kim SJ, Kim Y-H, Noh J-R, Gang G-T, Chung BH et al (2012) Susceptibility to gold nanoparticle-induced hepatotoxicity is enhanced in a mouse model of nonalcoholic steatohepatitis. *Toxicology* 294:27–35
24. Badawi NM, Teaima MH, El-Say KM, Attia DA, El-Nabarawi MA, Elmazar MM (2018) Pomegranate extract-loaded solid lipid nanoparticles: design, optimization, and in vitro cytotoxicity study. *Int J Nanomed* 13:1313
25. Stella B, Peira E, Dianzani C, Gallarate M, Battaglia L, Gigliotti CL et al (2018) Development and characterization of solid lipid nanoparticles loaded with a highly active doxorubicin derivative. *Nanomaterials* 8:110
26. Baek J-S, Na Y-G, Cho C-W (2018) Sustained cytotoxicity of wogonin on breast cancer cells by encapsulation in solid lipid nanoparticles. *Nanomaterials* 8:159
27. Wang W, Chen T, Xu H, Ren B, Cheng X, Qi R et al (2018) Curcumin-loaded solid lipid nanoparticles enhanced anticancer efficiency in breast cancer. *Molecules* 23:1578
28. Niu G, Yin S, Xie S, Li Y, Nie D, Ma L et al (2011) Quercetin induces apoptosis by activating caspase-3 and regulating Bcl-2 and cyclooxygenase-2 pathways in human HL-60 cells. *Acta Biochim Biophys Sin* 43:30–37
29. Zhao W, Li H, Hou Y, Jin Y, Zhang L (2019) Combined administration of poly-ADP-ribose polymerase-1 and caspase-3 inhibitors alleviates neuronal apoptosis after spinal cord injury in rats. *World Neurosurg* 127:e346–e352
30. Vijayakumar A, Baskaran R, Jang YS, Oh SH, Yoo BK (2017) Quercetin-loaded solid lipid nanoparticle dispersion with improved physicochemical properties and cellular uptake. *AAPS PharmSciTech* 8:875–883
31. Abbasalipourkabir R, Salehzadeh A, Abdullah R (2011) Delivering tamoxifen within solid lipid nanoparticles. *Pharm Technol* 35:74–79
32. Nie S, Hsiao WL, Pan W, Yang Z (2011) Thermoreversible pluronic F127-based hydrogel containing liposomes for the controlled delivery of paclitaxel: in vitro drug release, cell cytotoxicity, and uptake studies. *Int J Nanomed* 6:151–166
33. Niazvand F, Orazizadeh M, Khorsandi L, Abbaspour M, Mansouri E, Khodadadi A (2019) Effects of quercetin-loaded nanoparticles on MCF-7 human breast cancer cells. *Medicina* 55:114
34. Lin Y-C, Tsai P-H, Lin C-Y, Cheng C-H, Lin T-H, Lee KP et al (2013) Impact of flavonoids on matrix metalloproteinase secretion and invadopodia formation in highly invasive A431-III cancer cells. *PLoS One* 8:e71903
35. Wu Q, Kroon PA, Shao H, Needs PW, Yang X (2018) Differential effects of quercetin and two of its derivatives, isorhamnetin and isorhamnetin-3-glucuronide, in inhibiting the proliferation of human breast-cancer MCF-7 cells. *J Agric Food Chem* 66:7181–7189
36. Li X, Zhou N, Wang J, Liu Z, Wang X, Zhang Q et al (2018) Quercetin suppresses breast cancer stem cells (CD44+/CD24-) by inhibiting the PI3K/Akt/mTOR-signaling pathway. *Life Sci* 196:56–62
37. Wang L, Wang S, Chen R, Wang Y, Li H, Wang Y et al (2014) Oridonin loaded solid lipid nanoparticles enhanced antitumor activity in MCF-7 cells. *J Nanomater*. <https://doi.org/10.1155/2014/903646>

38. Wang L, Li H, Wang S, Liu R, Wu Z, Wang C et al (2014) Enhancing the antitumor activity of berberine hydrochloride by solid lipid nanoparticle encapsulation. *AAPS PharmSciTech* 15:834–844
39. Zhuang Y-G, Xu B, Huang F, Wu J-J, Chen S (2012) Solid lipid nanoparticles of anticancer drugs against MCF-7 cell line and a murine breast cancer model. *J Pharm Sci* 67:925–929
40. Sun M, Nie S, Pan X, Zhang R, Fan Z, Wang S et al (2014) Quercetin-nanostructured lipid carriers: characteristics and anti-breast cancer activities in vitro. *Colloids Surf B Biointerfaces* 113:15–24
41. Fulda SJ (2009) Tumor resistance to apoptosis. *Int J Cancer* 124:511–515
42. Naumov GN, Akslen LA, Folkman J (2006) Role of angiogenesis in human tumor dormancy: animal models of the angiogenic switch. *Cell Cycle* 5:1779–1787
43. Jain AK, Thanki K, Jain S (2014) Novel self-nanoemulsifying formulation of quercetin: implications of pro-oxidant activity on the anticancer efficacy. *Nanomed Biol Med* 10:e959–e969
44. Boots AW, Wilms LC, Swennen EL, Kleinjans JC, Bast A, Haenen GR (2008) In vitro and ex vivo anti-inflammatory activity of quercetin in healthy volunteers. *Nutrition* 24:703–710
45. Duan J, Mansour HM, Zhang Y, Deng X, Chen Y, Wang J et al (2012) Reversion of multidrug resistance by co-encapsulation of doxorubicin and curcumin in chitosan/poly (butyl cyanoacrylate) nanoparticles. *Int J Pharm* 426:193–201
46. Haghiaei M, Walle T (2005) Quercetin induces necrosis and apoptosis in SCC-9 oral cancer cells. *Nutr Cancer* 53:220–231
47. Lee D-H, Szczepanski M, Lee Y (2008) Role of bax in quercetin-induced apoptosis in human prostate cancer cells. *Biochem Pharmacol* 75:2345–2355
48. Duo J, Ying G-G, Wang G-W, Zhang L (2012) Quercetin inhibits human breast cancer cell proliferation and induces apoptosis via Bcl-2 and bax regulation. *Mol Med Rep* 5:1453–1456
49. Seo H-S, Ku JM, Choi H-S, Choi YK, Woo J-K, Kim M et al (2016) Quercetin induces caspase-dependent extrinsic apoptosis through inhibition of signal transducer and activator of transcription 3 signaling in HER2-overexpressing BT-474 breast cancer cells. *Oncol Rep* 36:31–42
50. Gao X, Wang B, Wei X, Men K, Zheng F, Zhou Y et al (2012) Anticancer effect and mechanism of polymer micelle-encapsulated quercetin on ovarian cancer. *Nanoscale* 4:7021–7030
51. Chaitanya GV, Alexander JS, Babu PP (2010) PARP-1 cleavage fragments: signatures of cell-death proteases in neurodegeneration. *Cell Commun Signal* 8:1–11
52. Herceg Z, Wang Z-Q (1999) Failure of poly (ADP-ribose) polymerase cleavage by caspases leads to induction of necrosis and enhanced apoptosis. *Mol Cell Biol* 19:5124–5133
53. Gobeil S, Boucher C, Nadeau D, Poirier G (2001) Characterization of the necrotic cleavage of poly (ADP-ribose) polymerase (PARP-1): implication of lysosomal proteases. *Cell Death Differ* 8:588–594
54. Yuan JJA (2009) Neuroprotective strategies targeting apoptotic and necrotic cell death for stroke. *Apoptosis* 14:469–477
55. Mohammadzadeh G (2021) Quercetin synergistically potentiates the anti-angiogenic effect of 5-fluorouracil on HUVEC cell line. *Mol Biol Rep*. <https://doi.org/10.21203/rs.3.rs-555480/v1>

**Publisher's Note** Springer Nature remains neutral with regard to jurisdictional claims in published maps and institutional affiliations.

Springer Nature or its licensor (e.g. a society or other partner) holds exclusive rights to this article under a publishing agreement with the author(s) or other rightsholder(s); author self-archiving of the accepted manuscript version of this article is solely governed by the terms of such publishing agreement and applicable law.